Computer Aided Geometric Design ••• (••••) •••–•••

Contents lists available at ScienceDirect

Computer Aided Geometric Design

www.elsevier.com/locate/cagd

Closed form inverse kinematics solution for a redundant anthropomorphic robot arm

Martin Pfurner

University of Innsbruck, Technikerstr. 13, 6020 Innsbruck, Austria

ARTICLE INFO

Article history:
Available online xxxx

Keywords:
Redundant manipulator
Anthropomorphic robot arm
Closed form solution

ABSTRACT

An inverse kinematics solution of a redundant 7R serial chain that mimics the human arm is presented. Such manipulators are composed of two spherical wrists with one revolute joint in between. In the case of non-redundant manipulators the inverse kinematics yields a discrete set of solutions for the joint axes to reach a given end effector position and orientation. For redundant arms, however, the solution consists of a one parameter set. In contrast to other solutions to this problem herein a closed form solution is given without the need of specifying the design, task nor the redundant parameter in the solution process. That gives the possibility to use the degree of freedom provided by the additional joint for different applications, such as avoiding singularities, joint limits and collisions or to apply an optimization algorithm to achieve, for example, minimal joint velocities or joint movements.

1. Introduction

The motivation for studying a redundant anthropomorphic robot arm was to compute a closed form inverse kinematic solution that gives the possibility to use all opportunities the redundancy of the arm enables. Herein the inverse kinematics, the task of computing the joint parameters to given task poses (position and orientation) in Cartesian space, is solved. Overall redundant manipulators offer many advantages over non-redundant ones that can be used in different ways to avoid singularities, joint limits or collisions.

As regards collision one may apply any of a variety of “envelope” intrusion detection techniques that surround actual links of the device, e.g., sphere “bubbles”. A specific example of these types of avoidance procedures is found in Ketchel and Larochelle (2004). Applying these to redundant manipulators is a two-edged sword. On one hand the manipulator is better equipped to avoid such problems. On the other, more collision, singularity or joint limit avoidance tests must be carried out, again, because of the extra links and joints. The inverse kinematics solution exposed herein permits parametric representation of separation distance so once a pose trajectory is selected it is possible to detect regions to be modified a-priori rather than carrying out detection computations repeatedly as discrete snap-shots along the way.

Furthermore a good closed form solution can be taken as a starting point for an optimization algorithm to reach, for example, minimal joint velocities or joint movements during a motion of the end effector system.

The manipulator dealt with in this article consists of two spherical wrists, each consisting of three perpendicular axes intersecting in one point, and a single revolute joint in between. Because of the fact, that in general six joints for a serial

E-mail address: martin.pfurner@uibk.ac.at.

http://dx.doi.org/10.1016/j.cagd.2016.05.008
0167-8396/

List of symbols

a_i	length of i-th link	**EE**	end effector matrix
d_i	offset on the i-th joint	t_i	entries of translation in **EE**
α_i	angle from joint i to $i+1$	a_{ij}	entries of rotation in **EE**
θ_i	joint angle of i-th joint	$\mathbf{M}_i$	rotation matrix of joint i
v_i	tangent half of θ_i	$\mathbf{G}_i$	DH transform. $i \to i+1$
W	wrist center point	e_i	rotation quaternion of **EE**
S	shoulder center point	E	center of elbow joint

Table 1
DH parameters of the robot.

i	a_i	d_i	α_i (deg)
1	0	0	90
2	0	0	90
3	0	d_3	90
4	0	0	90
5	0	d_5	90
6	0	0	90
7	0	0	0

manipulator would be enough to handle the Cartesian six degrees of freedom this manipulator with seven revolute axes is redundant. Its inverse kinematics can be divided into two tasks, a positioning and an orientational part, similarly to the solutions for wrist partitioned 6R manipulators shown in Angeles (1997), Pfurner (2009) and for the positioning part in Zsombor-Murray and Gfrerrer (2009).

There exist procedures to solve the inverse kinematics, for example presented in Moore and Oztop (2010) or in Wang and Artemiadis (2013). Similarly in Dahm and Joublin (1997), Asfour and Dillmann (2003) or in Singh and Claassens (2010) different methods for the solution of the inverse kinematics were applied but on a slightly different design in each case. In Al-Faiz et al. (2011) a combination of an analytical and a nonlinear optimization was used to solve the problem. Most of the articles concerning the issue of inverse kinematics of these types of manipulators apply numerical algorithms to the problem, but herein the approach is symbolic.

Using methods presented in aforementioned works one must substitute a numerical value for the redundant parameter throughout the solution algorithm to achieve discrete solutions for the inverse kinematics task. To the best of the authors knowledge this is the first time where a complete solution is presented without the need of setting a redundancy parameter to a special value before calculating the final solution.

This paper will proceed as follows. Section 2 shows the manipulator architecture to be considered. Section 3, together with its subsections, deal with the inverse kinematics solution. To demonstrate the power of this solution Section 4 gives numerical examples. Section 5 contains conclusions and suggests extension to this work including some problems that remain in this regard.

2. Manipulator geometry

The design of the manipulator is given by Denavit Hartenberg (DH) (Denavit and Hartenberg, 1955) parameters as shown in Table 1.

All axes of the revolute joints are perpendicular to the adjacent ones. The origin of the base frame (x_b, y_b, z_b) is centered in the first wrist center point (intersection of axes one, two and three) and the z-axis coincides with the first axis. The x-axis lies perpendicular to the plane spanned by the first and second axis in the home position, i.e., where all joint parameters are equal to zero. In this configuration all axes lie in the yz plane. The origin of the end effector (x_e, y_e, z_e) frame is chosen on the second wrist center (intersection of axes five, six and seven), the z-axis coincides with axis seven and the x-axis is perpendicular to the plane spanned by axes six and seven in the home position. Because of this special choice of the end effector frame the last row of Table 1 is zero. This entry is nevertheless retained in the table to permit consistent formulation of symbolic expressions to be introduced here. A pictorial schematic of the manipulator is given in Fig. 1, left side. Note that in this home configuration the axes of joints one and three as well as the axes of joints five and seven coincide.

Without loss of generality one can always choose this base and end effector frame. Other choices invoke transformations of the manipulators reference frame and the given end effector pose only and do not effect the solution but incur unnecessary computation. These changes of the frames can be embedded into the given end effector pose to achieve the starting point of these calculations.

Instead of the joint angles θ_i sometimes the corresponding algebraic value, using the tangent half angle substitution $v_i = \tan(\frac{\theta_i}{2})$, is used.

Please cite this article in press as: Pfurner, M. Closed form inverse kinematics solution for a redundant anthropomorphic robot arm. Comput. Aided Geom. Des. (2016), http://dx.doi.org/10.1016/j.cagd.2016.05.008

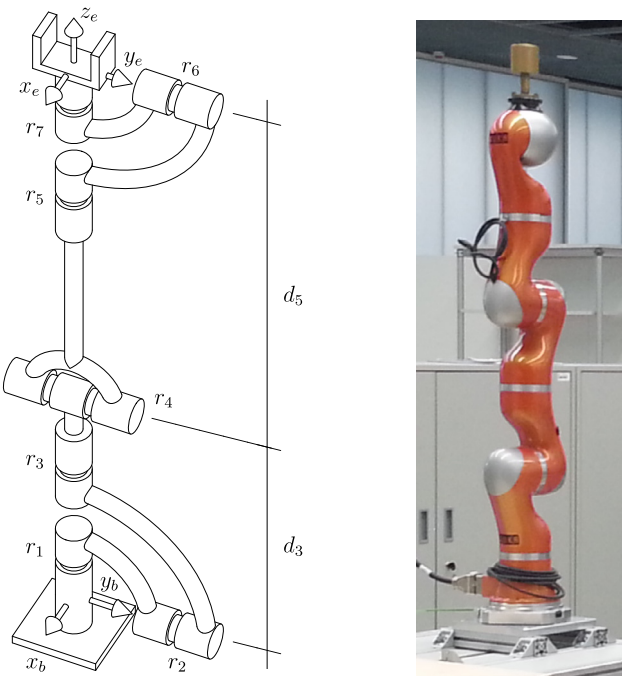

Fig. 1. Schematic sketch and picture of the manipulator in the home configuration.

The redundancy of this special anthropomorphic robot arm is the rotation around the axis connecting the two wrist center points. In an arbitrary redundant 7R manipulator all six degrees of freedom would remain even if one of the revolute axes is blocked. In contrast the redundancy of this special manipulator is degenerated. It looses a degree of freedom by blocking the fourth revolute joint, which would constrain the wrist center point to move on a sphere. In the following sections this manipulator will be analyzed.

3. Inverse kinematics

The inverse kinematics is the problem of mapping the task of the robot in Cartesian space into the joint space such that the robot can reach the given end effector pose using the joint values thus obtained.

The end effector pose with respect to the base frame is given by

$$\mathbf{EE} = \begin{pmatrix} 1 & 0 & 0 & 0 \\ t_1 & a_{11} & a_{12} & a_{13} \\ t_2 & a_{21} & a_{22} & a_{23} \\ t_3 & a_{31} & a_{32} & a_{33} \end{pmatrix}, \tag{1}$$

where the first column is the translational part and the lower right 3×3 matrix is a proper orthogonal matrix and gives the orientation of the end effector frame with respect to the base frame.

Then the problem of the inverse kinematics is to solve the matrix equation

$$\prod_{i=1}^{7} \mathbf{M}_i(\theta_i)\mathbf{G}_i(a_i) = \mathbf{EE} \tag{2}$$

with

$$\mathbf{M}_i = \begin{pmatrix} 1 & 0 & 0 & 0 \\ 0 & \cos(\theta_i) & \sin(\theta_i) & 0 \\ 0 & -\sin(\theta_i) & \cos(\theta_i) & 0 \\ 0 & 0 & 0 & 1 \end{pmatrix} \tag{3}$$

and

$$\mathbf{G}_i = \begin{pmatrix} 1 & 0 & 0 & 0 \\ a_i & 1 & 0 & 0 \\ 0 & 0 & \cos(\alpha_i) & \sin(\alpha_i) \\ d_i & 0 & -\sin(\alpha_i) & \cos(\alpha_i) \end{pmatrix}. \tag{4}$$

Please cite this article in press as: Pfurner, M. Closed form inverse kinematics solution for a redundant anthropomorphic robot arm. Comput. Aided Geom. Des. (2016), http://dx.doi.org/10.1016/j.cagd.2016.05.008

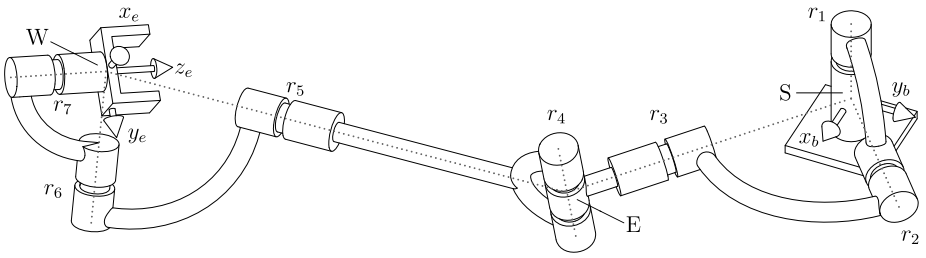

Fig. 2. Manipulator in an arbitrary configuration. The dotted lines show the axes of the revolute joints.

The robot under consideration is a combination of two spherical wrists, i.e., two times three mutually intersecting revolute joints and an additional revolute one, joint four, between them to handle the distance of the two wrist center points. Subsequently we will call the two spherical joints 'shoulder' and 'wrist' whereas the intermediate revolute joint will be called 'elbow'. The centers of shoulder and wrist will be denoted by S and W and the common point of axes 3, 4 and 5 by E (see Fig. 2).

By reformulating Eq. (2) as

$$\mathbf{M}_1\mathbf{G}_1\mathbf{M}_2\mathbf{G}_2\mathbf{M}_3\mathbf{G}_3\mathbf{M}_4\mathbf{G}_4 = \mathbf{E}\mathbf{E}\,\mathbf{G}_7^{-1}\mathbf{M}_7^{-1}\mathrm{G}_6^{-1}\mathbf{M}_6^{-1}\mathbf{G}_5^{-1}\mathbf{M}_5^{-1} \tag{5}$$

one splits the manipulator in two parts. The left hand side is a 4R-chain, fixed in the base frame of the initial robot, and the right hand side is a spherical wrist fixed in the prescribed end effector pose. The left part takes care of the correct positioning of the point W and the right part carries out the orientational task. Therefore the inverse kinematics can be divided into a positional task using axes one to four and an orientational task by using the remaining three axes.

The following subsections will show the solution process for the inverse kinematics problem of the prescribed mechanism in a sequence, but the solution at the end will be implicit equations for the joint angles depending on an arbitrary design, end effector and redundancy parameter, i.e., without setting any numerical value.

3.1. Joint angle four

Because only r_4 can alters the distance between wrist centers this joint angle can be computed immediately via triangle SEW. If a pose is given all side length of this triangle are known and the tangent half angle of joint four can be calculated using the formula

$$\tan\frac{\alpha}{2} = \pm\sqrt{\frac{(s-b)(s-c)}{s(s-a)}}, \tag{6}$$

where s is half of the triangle circumference, a, b and c are the lengths of its edges and α is the angle opposite to side a. Therefore revolute angle four can be derived as

$$v_4 = \pm\sqrt{-\frac{d_3^2 - 2d_3d_5 + d_5^2 - t_1^2 - t_2^2 - t_3^2}{d_3^2 + 2d_3d_5 + d_5^2 - t_1^2 - t_2^2 - t_3^2}}, \tag{7}$$

where d_3 is the offset on the third and d_5 the offset on the fifth axis.

3.2. Joint angles one, two and three

After having adjusted the distance of wrist and shoulder by means of v_4 the next task is to guide the wrist center to its desired position using the first three revolute axes. Geometrically this means to position W on a sphere. Here the redundancy has to be taken into account because for the two degrees of freedom of the task three axes can be used.

Therefore the value of the position of the origin of the moving frame (depending on the first three joint angles v_i, $i = 1, 2, 3$), together with the desired position, yields a redundant system of three equations in three unknowns. Using this special choice of base coordinate frame the third equation, which is in fact the equation for the z-value of the position, is independent of v_1. This is clear because this joint only rotates around the z-axis and has therefore no influence on the z-value of any point of the manipulator. Using this equation it is possible to compute one of the two angles v_2 or v_3 in dependency on the other one. Without loss of generality we will consider the second joint value v_2 as the free parameter (vice versa one could also compute v_2 as function of v_3) and compute v_3 as

$$v_3(v_2) = \pm\sqrt{-\frac{k_1 + 4d_5v_2v_4}{k_1 - 4d_5v_2v_4}} \tag{8}$$

where

Please cite this article in press as: Pfurner, M. Closed form inverse kinematics solution for a redundant anthropomorphic robot arm. Comput. Aided Geom. Des. (2016), http://dx.doi.org/10.1016/j.cagd.2016.05.008

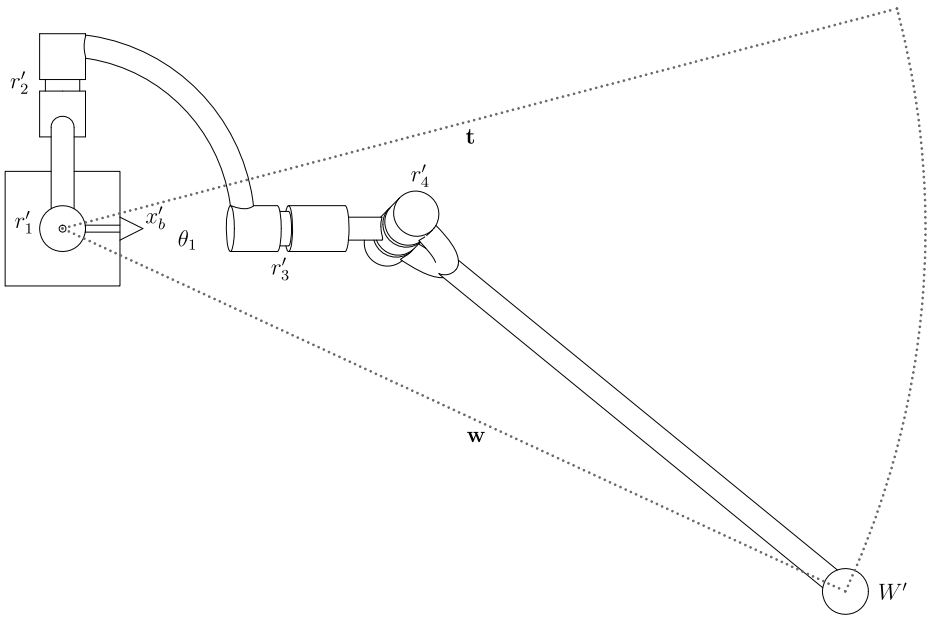

Fig. 3. Top view of the partial solution of angles two, three and four.

$$k_1 = v_2^2 v_4^2(d_3 + d_5 - t_3) + v_2^2(d_3 - d_5 - t_3) + v_4^2(-d_3 - d_5 - t_3) - d_3 + d_5 - t_3. \tag{9}$$

For a discrete value of v_2 Eq. (8) gives for each value of v_4 two values of v_3 which only differ in the sign. As one can see in Eqs. (8) and (9) the negative value of v_4, to the same value of v_2, causes the reciprocal values of v_3.

Depending on the free parameter v_2 and the solution for angle v_3 in Eq. (8) the first revolute angle can be calculated. For this purpose one can substitute the solutions of angles two to four into the forward kinematics of the first four axes (left hand side of Eq. (5)) and set the first revolute angle to zero. The angle in the top view between the rays

$$\mathbf{w} = \frac{2v_2 d_3}{v_2^2+1} + \left(\frac{2(1-v_2^2)(-v_3^2+1)v_4}{(v_2^2+1)(v_3^2+1)(v_4^2+1)} - \frac{2v_2(1-v_4^2)}{(v_2^2+1)(v_4^2+1)} \right) d_5 - \frac{4v_3 v_4 d_5}{(v_4^2+1)(v_3^2+1)} \tag{10}$$

pointing from the origin to this position W and the desired position $\mathbf{t} = [t_1, t_2]^T$ is exactly the revolute angle of the first joint, like shown in Fig. 3. This yields

$$v_1(v_2) = \frac{4v_3 v_4 d_5 (v_2^2+1)(\sqrt{t_1^2+t_2^2}+t_1) + t_2 k_2}{-4v_3 v_4 d_5 t_2 (v_2^2+1) + k_2(\sqrt{t_1^2+t_2^2}+t_1)} \tag{11}$$

with

$$k_2 = \sqrt{t_1^2+t_2^2}(v_2^2+1)(v_3^2+1)(v_4^2+1) + 2v_4 d_5(1-v_3^2)(1-v_2^2) + 2(v_3^2+1)v_2(d_3(v_4^2+1) + d_5(1-v_4^2)). \tag{12}$$

If W is located on the axis of the first revolute joint, meaning $t_1 = t_2 = 0$, Eq. (11) does not yield a valid solution. In this special case the angle for the first revolute axis is not determined uniquely and can be chosen arbitrarily. This gives an additional degree of freedom in this special case. If W is located on the axis of the third revolute joint $v_4 \to \infty$ which means that the angle of the fourth revolute joint is equal to π. This additionally implies that the axes of the third and the fifth joint are aligned. In such a configuration the manipulator's arm is in a stretched position, where v_3 can be chosen arbitrarily. In general cases Eqs. (7), (8) and (11) yield four one parameter sets of solutions to guide point W in the desired position given by the first column of the end effector matrix in Eq. (1). The parameter v_2 can, at least theoretically vary in the range $(-\infty, \infty)$, which corresponds to the range $(-\pi, \pi)$ for the joint angle θ_2, or practically within its joint limits.

On the other hand Eq. (8) defines for every value of v_4 two explicit curves in the $v_2 v_3$ plane, altogether 4 curves. Because of the structure of this explicit equation the real parts of the two implicit curves to the same sign of v_4 meet at the v_2 axis and are reflections of each other with respect to the same axis. By taking the square of Eq. (8) one can eliminate the radical to get

$$k_1(v_3^2+1) - 4d_5 v_2 (v_3^2-1)v_4 = 0, \tag{13}$$

with k_1 defined in Eq. (9). Therefore for a given value of v_4 this single algebraic curve describes the relation between v_2 and v_3.

Please cite this article in press as: Pfurner, M. Closed form inverse kinematics solution for a redundant anthropomorphic robot arm. Comput. Aided Geom. Des. (2016), http://dx.doi.org/10.1016/j.cagd.2016.05.008

3.3. Joint angles five, six and seven

In the third step one has to substitute the solution for the first four joint angles computed in Subsections 3.1–3.3 in the forward kinematics of the chain determined by the first four axes to achieve

$$\mathbf{M}_1\mathbf{G}_1\mathbf{M}_2\mathbf{G}_2\mathbf{M}_3\mathbf{G}_3\mathbf{M}_4\mathbf{G}_4 = \mathbf{F}\mathbf{W}_4. \tag{14}$$

Then Eq. (2) can be rewritten in the form

$$\mathbf{M}_5\mathbf{G}_5\mathbf{M}_6\mathbf{G}_6\mathbf{M}_7\mathbf{G}_7 = \mathbf{F}\mathbf{W}_4^{-1}\mathbf{E}\mathbf{E}. \tag{15}$$

This matrix equation is the mathematical description of the inverse kinematics of a spherical canonical 3R-chain, meaning that the common point of intersection is positioned in the center of the base frame and the moving frame, which coincide. Using the theory in Husty et al. (2007) it is possible to compute the solutions to this problem right away as

$$\begin{aligned} v_5 &= \frac{e_0e_2 + e_1e_3 \pm \sqrt{(e_1^2+e_2^2)(e_0^2+e_3^2)}}{e_0e_1 - e_2e_3},\ v_6 = \mp\frac{\sqrt{(e_1^2+e_2^2)(e_0^2+e_3^2)}}{e_1^2+e_2^2}, \\ v_7 &= \frac{(-e_0e_2 + e_1e_3 \pm \sqrt{(e_1^2+e_2^2)(e_0^2+e_3^2)}}{e_0e_1 + e_2e_3}, \end{aligned} \tag{16}$$

where (e_0, e_1, e_2, e_3) is a quaternion representing the rotational part of $FW_4^{-1}EE$. In the special case of $e_1 = e_2 = 0$, which means a pure rotation around the z-axis of the base frame, these formulas have to be adapted because they do not yield valid solutions. This can be done using the theory in Husty et al. (2007). To every solution for the first four joint angles of the manipulator one achieves one matrix equation like Eq. (15). This yields two solutions for the remaining joint angles in Eq. (16). Therefore for a discrete value of the redundancy parameter v_2 one achieves up to eight real solutions for the inverse kinematics problem.

4. Numerical example

First of all a design has to be fixed. Choosing $d_3 = 3$ and $d_5 = 5$ the upper and forearm are established.

4.1. Solution to a discrete pose

To be certain that the algorithm yields correct solutions it is always advisable to start with a known solution obtained via direct kinematics and use that end effector pose as a test of the inverse kinematic procedure. But that is only the first step. The whole set of solutions is verified by substitution in the forward kinematics to reach the prescribed end effector pose. Here this known solution

$$v_1 = -\frac{1}{91},\ v_2 = \frac{7}{11},\ v_3 = \frac{1}{5},\ v_4 = \frac{11}{7},\ v_5 = \frac{1}{3},\ v_6 = 23,\ v_7 = \frac{13}{17} \tag{17}$$

yields the end effector pose

$$\mathbf{E}\mathbf{E} = \begin{pmatrix} 1 & 0 & 0 & 0 \\ \frac{99055033}{15557737} & \frac{85256419116}{944121269845} & \frac{2908270221593}{4720606349225} & \frac{948838668}{1212588325} \\ -\frac{146433441}{77788685} & \frac{-152385564777}{188824253969} & \frac{477406432716}{944121269845} & -\frac{73965584}{242517665} \\ \frac{30432}{18785} & -\frac{133051168}{227993545} & -\frac{688479564}{1139967725} & \frac{158961}{292825} \end{pmatrix}. \tag{18}$$

Substitution of the design and end effector pose Eq. (18) into the solutions given by Eqs. (11), (8), (7) and (16) yield all the one parameter sets of solutions to this discrete end effector pose. One of these solutions is

$$\begin{aligned} v_1 &= \frac{272076123v_3v_2^2 - 704673970v_3v_2 - 524113947v_3 - 292866882v_2}{272076123v_2^2 + 990550330v_2 + 524113947}, \\ v_3 &= -\sqrt{-\frac{65703v_2^2 + 170170v_2 - 126567}{65703v_2^2 - 170170v_2 - 126567}}, \qquad v_4 = \frac{11}{7}, \end{aligned} \tag{19}$$

however the equations for v_5, v_6 and v_7 are too long to be useful. Each solution set corresponds to implicit curves in the joint parameter spaces $v_i(v_2)$, $i \in [1, 3, 4, 5, 6, 7]$. All these curves are drawn in Fig. 4, where the angles are measured in radians and the vertices of the surrounding boxes mark the values of $\pm\pi$ to each angle, which means that for each quadrangle the top and the bottom as well as the left and the right vertices have to be identified. In all of these six plots the horizontal axis is the θ_2 axis. They have to be read in the following manner: to the given end effector pose

Please cite this article in press as: Pfurner, M. Closed form inverse kinematics solution for a redundant anthropomorphic robot arm. Comput. Aided Geom. Des. (2016), http://dx.doi.org/10.1016/j.cagd.2016.05.008

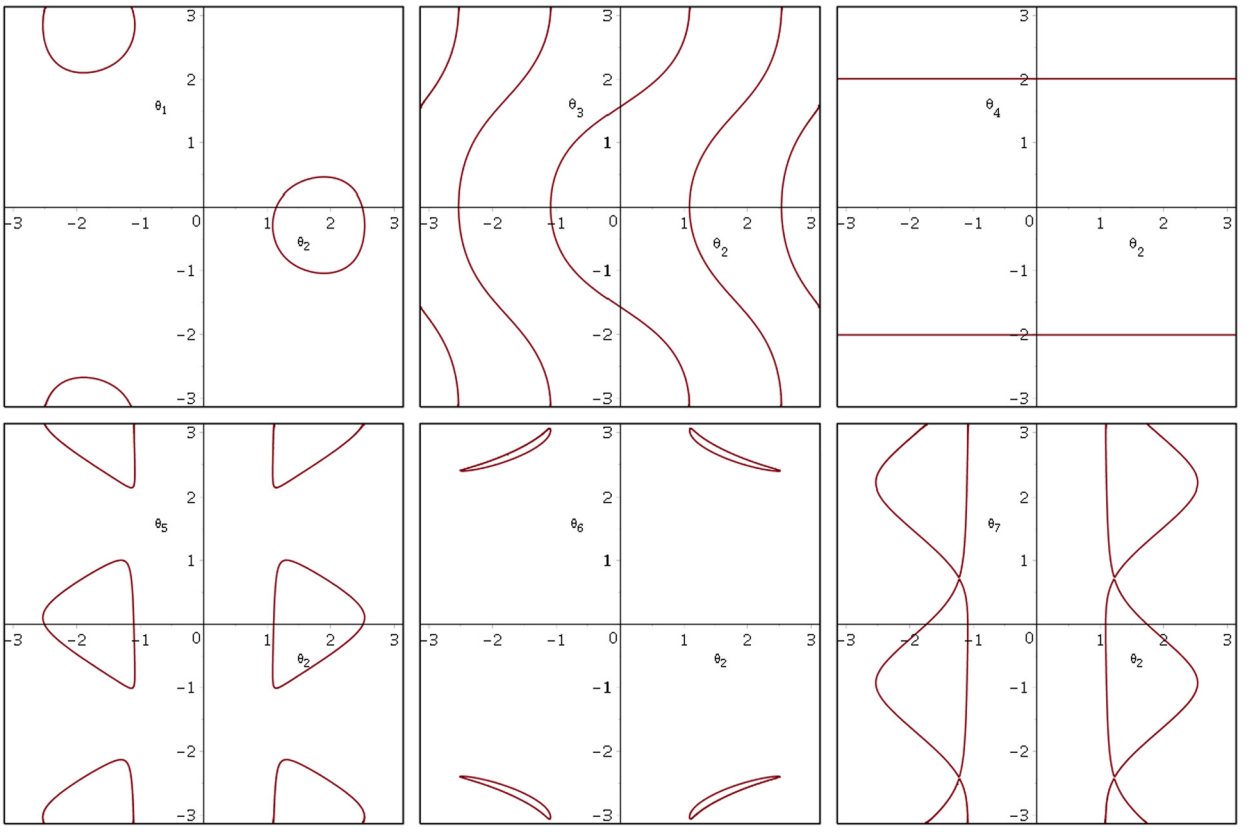

Fig. 4. All one parameter solutions $\theta_i(\theta_2)$ in radians, for $i = 1, 3, 4$ in the first row and $i = 5, 6, 7$ in the second row.

Table 2
All solutions with assumption $v_2 = \frac{7}{11}$ with $w_1 = \sqrt{7487252803099413873769}$.

Nr.	v_1	v_3	v_4	v_5	v_6	v_7
1	$-\frac{20119}{70904}$	$-\frac{1}{5}$	$\frac{11}{7}$	$\frac{201464672}{319666665} - \frac{w_1}{73203666285}$	$\frac{w_1}{9519168409}$	$-\frac{75903633555-w_1}{41543846912}$
2	$-\frac{20119}{70904}$	$-\frac{1}{5}$	$\frac{11}{7}$	$\frac{201464672}{319666665} + \frac{w_1}{73203666285}$	$-\frac{w_1}{9519168409}$	$-\frac{75903633555+w_1}{41543846912}$
3	$-\frac{1}{91}$	$\frac{1}{5}$	$\frac{11}{7}$	$\frac{1}{3}$	23	$\frac{13}{17}$
4	$-\frac{1}{91}$	$\frac{1}{5}$	$\frac{11}{7}$	-3	-23	$-\frac{17}{13}$
5	$-\frac{1}{91}$	-5	$-\frac{11}{7}$	-3	23	$\frac{13}{17}$
6	$-\frac{1}{91}$	-5	$-\frac{11}{7}$	$\frac{1}{3}$	-23	$-\frac{17}{13}$
7	$-\frac{20119}{70904}$	5	$-\frac{11}{7}$	$\frac{201464672}{319666665} + \frac{w_1}{73203666285}$	$\frac{w_1}{9519168409}$	$-\frac{75903633555-w_1}{41543846912}$
8	$-\frac{20119}{70904}$	5	$-\frac{11}{7}$	$\frac{201464672}{319666665} - \frac{w_1}{73203666285}$	$-\frac{w_1}{9519168409}$	$-\frac{75903633555+w_1}{41543846912}$

in Eq. (18) all solutions for a given θ_2 can be found by intersecting these curves in Fig. 4 with the line $\theta_2 = const$. Of course in this direction by using the intersection of the curves one has to figure out which intersection in the first plot corresponds to which intersection in the second plot and so on, whereas the formulas in Section 3 yield, of course, the correct corresponding tuples for the solution.

To achieve the starting and all corresponding solutions we have to substitute $v_2 = \frac{7}{11}$ into Eqs. (19) or, on the other hand, intersect the curves in Fig. 4 with the corresponding line to the angle $\theta_2 = 22.62°$. All solutions are shown in Table 2.

4.2. Solution to a motion of the end effector

Maybe the greatest advantage of this inverse kinematics solution is that the end effector pose is general. Therefore it is also possible to compute the joint angles to a given motion of the end effector. For example the matrix

Please cite this article in press as: Pfurner, M. Closed form inverse kinematics solution for a redundant anthropomorphic robot arm. Comput. Aided Geom. Des. (2016), http://dx.doi.org/10.1016/j.cagd.2016.05.008

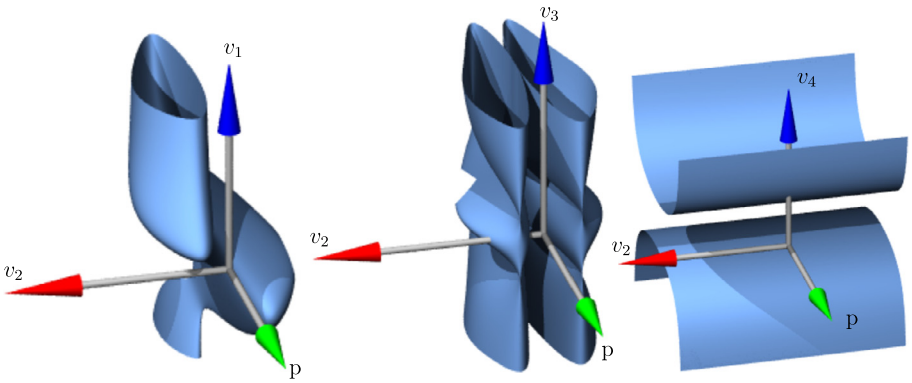

Fig. 5. Solutions to a one parameter motion of the end effector for $v_1(v_2, p)$ (left), $v_3(v_2, p)$ (middle), $v_4(p)$ (right).

$$\mathbf{EE}_{motion} = \begin{pmatrix} 1 & 0 & 0 & 0 \\ p & 1 & 0 & 0 \\ p+7 & 0 & 1 & 0 \\ \frac{1}{2}p-1 & 0 & 0 & 1 \end{pmatrix} \tag{20}$$

represents a linear motion of the origin of the end effector where the orientation is equal to the identity. This relatively simple motion was chosen to offer the possibility to show some of the solutions. It has to be noted that any motion in matrix form could be substituted in the closed form solution, but the resulting equations would become quite unwieldy.

Substitution of Eq. (20) into Eqs. (11), (8), (7) and (16) yield the explicit solutions

$$\begin{aligned} v_1(v_2, p) = {} & (9p^2v_2^2w_2 + 18p^2v_2v_4w_2 + 40pv_2^2w_2 + 104pv_2v_4w_2 - 9p^2w_2 + \\ & 160v_2^2w_2 - 112v_2v_4w_2 + 48pv_2 - 64pw_2 + 336v_2 - 112w_2)/ \\ & (9p^2v_2^2 + 40pv_2^2 + 9p^2 + 48pv_2 + 160v_2^2 + 64p + 112) \end{aligned} \tag{21}$$

with

$$\begin{aligned} w_2 = {} & \sqrt{-(9p^2v_2^2 - 18p^2v_2v_4 + 40pv_2^2 - 104pv_2v_4 - 9p^2 + 160v_2^2 + } \\ & \overline{112v_2v_4 - 64p - 112)/(9p^2v_2^2 + 18p^2v_2v_4 + 40pv_2^2 + 104pv_2v_4 - } \\ & \overline{9p^2 + 160v_2^2 - 112v_2v_4 - 64p - 112)} \\ v_3(v_2, p) = {} & \sqrt{-(9p^2v_2^2 - 18p^2v_2v_4 + 40pv_2^2 - 104pv_2v_4 - 9p^2 + 160v_2^2 + } \\ & \overline{112v_2v_4 - 64p - 112)/(9p^2v_2^2 + 18p^2v_2v_4 + 40pv_2^2 + 104pv_2v_4 - } \\ & \overline{9p^2 + 160v_2^2 - 112v_2v_4 - 64p - 112)} \end{aligned} \tag{22}$$

and

$$v_4(t) = \sqrt{-\frac{9p^2 + 52p + 184}{9p^2 + 52p - 56}}. \tag{23}$$

These Eqs. (21), (22) and (23) are implicit representations of surfaces in the three dimensional space defined by the coordinates v_i, v_2 and t for $i = 1, 3, 4$. Fig. 5 shows these surfaces for $v_1(v_2, p)$, $v_3(v_2, p)$ and $v_4(v_2, p)$ from left to right.

To follow this motion, where p varies in $[p_0, p_1]$ one has the possibility to choose a curve on one of the surfaces $v_i(v_2, p)$, $i \in [1, 3, 4, 5, 6, 7]$, with a starting point in the plane $p = p_0$ and an endpoint in the plane $p = p_1$. If the mechanism should pass the motion with an increasing or strictly increasing parameter p these curves should also be defined in a way with an increasing or strictly increasing parameter p. For simplicity the curve could be defined by the implicit parameterization $v_2 = v_2(p)$, which immediately induces a curve on each of the surfaces. The solutions to the inverse kinematics problem along this path is then given by the curves $v_i(v_2(p), p)$. A change of the parameterization of $v_2 = v_2(p)$ admits the possibility to vary the configuration during the motion.

5. Conclusion

A new and efficient algorithm for the solution of the inverse kinematics problem of a redundant anthropomorphic robot arm has been revealed herein. It yields a complete closed form solution such that the design and, much more important,

Please cite this article in press as: Pfurner, M. Closed form inverse kinematics solution for a redundant anthropomorphic robot arm. Comput. Aided Geom. Des. (2016), http://dx.doi.org/10.1016/j.cagd.2016.05.008

the end effector pose remains general. This provides the opportunity to achieve joint functions depending on the redundancy and motion parameter of the end effector. This feature can be used in multiple applications, for example in collision avoidance, in motion planning for preventing to run into joint limits or to optimize motion of the mechanism for given paths. This article only provides the theoretical tool for solving the inverse kinematics problem of the robot arm. This algorithm will be used in an application involving two such SRS robots executing intricate planned tasks so as to exploit the capabilities offered by redundancy.

References

Al-Faiz, M.Z., Ali, A.A., Miry, A.H., 2011. Human arm inverse kinematic solution based geometric relations and optimization algorithm. Int. J. Robot. Autom. 2 (4), 245–255.

Angeles, J., 1997. Fundamentals of Robotic Mechanical Systems. Theory, Methods and Algorithms. Springer, New York.

Asfour, T., Dillmann, R., 2003. Human-like motion of a humanoid robot arm based on a closed-form solution of the inverse kinematics problem. In: Int. Conf. on Intelligent Robots and Systems. IROS, Las Vegas, Nevada, USA, pp. 1407–1412.

Dahm, P., Joublin, F., 1997. Closed form solution for the inverse kinematics of a redundant robot arm. Tech. Rep. 08. Institut für Neuroinformatik, Ruhr-Universität Bochum, Germany.

Denavit, J., Hartenberg, R.S., 1955. A kinematic notation for lower-pair mechanisms based on matrices. J. Appl. Mech. 22, 215–221.

Husty, M.L., Pfurner, M., Schröcker, H.-P., 2007. Algebraic methods in mechanism analysis and synthesis. Robotica 25 (6), 661–675.

Ketchel, J.S., Larochelle, P.M., 2004. Line based collision detection of cylindrical rigid bodies. In: 28th Biennial Mechanisms and Robotics Conference, Parts A and B, vol. 2. ASME, Salt Lake City, Utah, pp. 1261–1271.

Moore, B., Oztop, E., 2010. Redundancy parameterization for flexible motion control. In: Proc. of IDETC/CIE. Montreal, Canada, pp. 1–8.

Pfurner, M., 2009. Explicit algebraic solution of geometrically simple serial manipulators. In: Proc. of the 5th Int. Workshop on Computational Kinematics. Springer, Berlin, Heidelberg, pp. 167–174.

Singh, G.K., Claassens, J., 2010. An analytical solution for the inverse kinematics of a redundant 7dof manipulator with link offsets. In: Int. Conf. on Intelligent Robots and Systems. IROS, Taipei, Taiwan, pp. 2976–2982.

Wang, Y., Artemiadis, P., 2013. Closed-form inverse kinematic solution for anthropomorphic motion in redundant robot arms. Adv. Robot. Autom. 2 (3). http://dx.doi.org/10.4172/2168-9695.1000110.

Zsombor-Murray, P., Gfrerrer, A., 2009. 3R wrist positioning – a classical problem and its geometric background. In: Proc. of the 5th Int. Workshop on Computational Kinematics. Springer, Berlin, pp. 175–182.

Please cite this article in press as: Pfurner, M. Closed form inverse kinematics solution for a redundant anthropomorphic robot arm. Comput. Aided Geom. Des. (2016), http://dx.doi.org/10.1016/j.cagd.2016.05.008